Switching magnetic waveguide on metasurface to delivering WPT and propulsion for an untethered micro-robot

Huu Nguyen Bui, Jong-Wook Lee*
Department of Electronics Engineering, Kyung Hee University
E-mail: jwlee@khu.ac.kr

With small dimensions, the operating time of an untethered micro-robot is limited by the small battery capacity. To perform critical missions for a long time, realizing stable power for the micro-robot is a major challenge. Recently, magnets are being replaced with a magnetically-coupled coil, which allows for the adoption of the wireless power transfer (WPT) technique. This approach provides a significant advantage of delivering both propulsion and power [1,2].

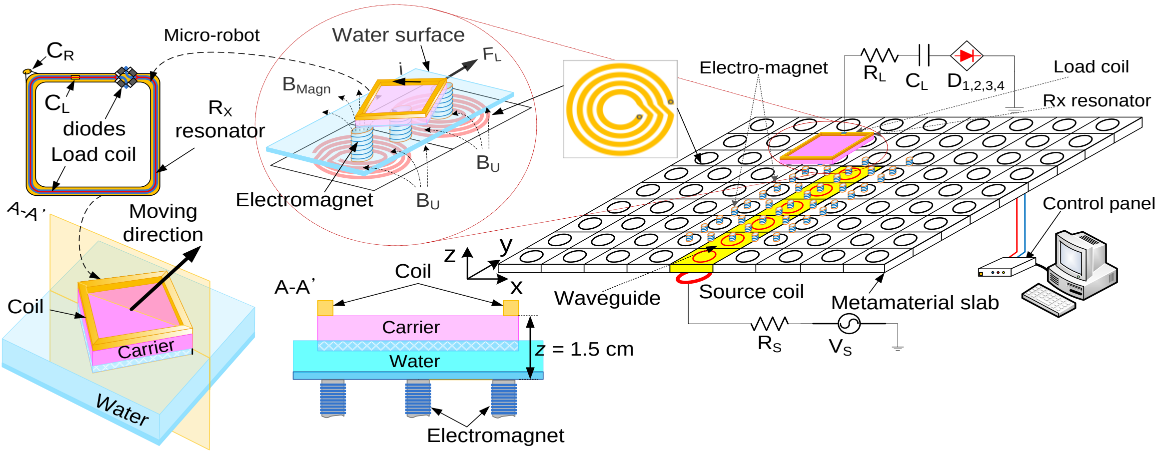

Fig.1. The structure of the propulsion system.

Kim et al. investigated WPT technology to generate a propulsion force and torque for the micro-robot [2]. One drawback of this approach is the microrobot do not operate at resonance region, which has a maximum WPT efficiency. Another issue is that the size and weight of the coil become rather large when a relatively low frequency of 20 kHz is used. In addition, the magnetic waves are leaky to the medium due to the different size of the Tx coil and microrobot. This limits the size reduction of the microrobot. Finally, the previous approach cannot directly control the direction of movement, which limits the ability to explore complex paths.

In this paper, we propose a new approach to provide a stable power source for an untethered tiny micro-robot. The approach is realized using a magnetic waveguide as an energy transferring channel enabled by the defect band created on the metasurface. Consequently, we can reduce leaky waves from source coil to the microrobot. Instead of a time-varying magnetic field, we use a static field generated from selectively activated electromagnets interacting with a full wave rectifier current on the microrobot to generate propulsion. Our overall system is shown in Fig. 1. The Lorentz force applies to the microrobot is calculated by

$$F_L = \frac{n_L}{T}\int_0^T (\boldsymbol{i}\times\boldsymbol{B}l)dt \cong n_L\left|\bar{B}\right|\left|\bar{i}\right| l = \frac{2n_L}{\pi}\left|B_{\mathrm{Magn}}\right|\left|I_{\mathrm{L}}\right| l_{\mathrm{Eff,side}}, \qquad (1)$$

where n_{L} is a number of turns, B_{Magn} is static magnetic flux density generated by electromagnet obtained using the method [3], $I_L = \sqrt{\eta P_S / R_L}$ is the current of the load coil depending on input power P_{S} and the WPT efficiency η, $l_{\mathrm{Eff,\ the\ side}}$ is the effective length of the microrobot depending on the length part contacted with B_{Magn}. Applying Newton's second law for ship movement, we obtain the second-order differential equation for the distance x(t) as

$$m\frac{d^2x}{dt^2} + \frac{1}{2}\rho C_{\mathrm{D}} S_{\mathrm{W}}\left(\frac{dx}{dt}\right)^2 - \left|F_{\mathrm{L}}(t)\right| = 0, \qquad (2)$$

where m is the mass of the microrobot, ρ is the density of the water, C_{D} is the drag (resistance) coefficient of the ship [2], and v is the velocity. $S_{\mathrm{W}} \cong 4\,(h_{\mathrm{Ship}} \times l_{\mathrm{Ship}}) + l^2_{\mathrm{Ship}}$ is the wetted area of the ship, which can be obtained using the sum of the side area and bottom area contacting the water. Fig. 2 shows the images of the microrobot towards a goal location.

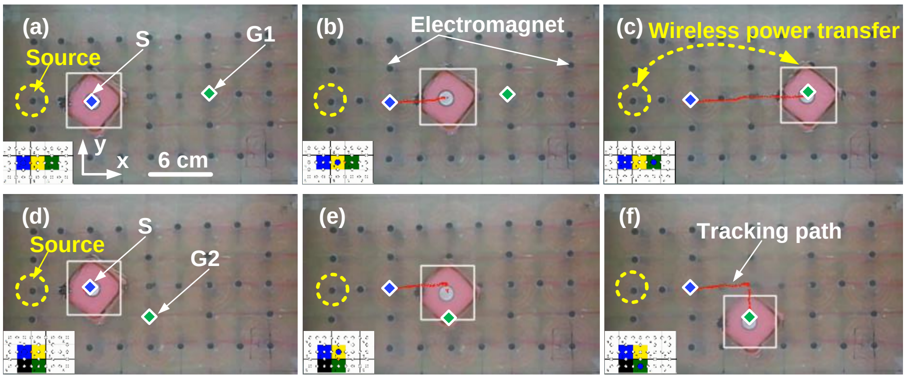

Fig. 2. Images of the micro-robot. (a) Initial scene with start (S) and goal (G1) locations, (b) robot following a selected path, (c) robot reaching the goal location, (d) robot starts at (S) and goal (G2) locations, (e) robot following a new path, (f) robot changing direction to reach the second goal (G2) location. Grid maps for pathfinding are shown in the insets. Start and goal locations are indicated with

Acknowledgments This research was supported by the Basic Science Research Program through the National Research Foundation of Korea (NRF-2018R1A2A2A05018621).

References [1] M. Karpelson, B. H. Waters, B. Goldberg, B. Mahoney, O. Ozcan, A. Baisch, P. M. Meyitang, J. R. Smith, and R. J. Wood, in 2014 IEEE International Conference on Robotics and Automation, pp. 2384–2391, Hong Kong, China, Sept. 2014. [2] D. Kim, K. Hwang, J. Park, H. Ho Park, and S. Ahn, IEEE Trans. Magn., vol. 53, no.6, pp. 9401804, June 2017. [3] H. N. Bui, T. S. Pham, V. Ngo, and J. W. Lee, J. App. Phys., vol. 122, no. 9, pp. 093102, Sept. 2017.